Novel Differential Protection Approach of UHV AC Transmission Lines Based on Tellegen's Quasi-Power Theorem

S. M. Liu, *Member, IEEE*, B. Wang, Y.S. Zhao, L. L. Zhang, *Member, IEEE*, and L. Jiang, *Member, IEEE*

***Abstract*-- When current differential protection is applied to an AC transmission line, synchronous sampling at the two ends is required. The use of GPS synchronization increases the difficulty and cost of project implementation while the use of 'ping-pong' synchronization requires that the communication channel has equal transmission and reception delay. To overcome the impact of these issues, power differential protection has been proposed. However, power differential protection cannot fully identify the fault zone for solid single-line-to-ground fault. This paper proposes a novel differential protection approach based on the Tellegen's quasi-power theorem. The approach retains the advantages of current differential protection. Meanwhile, it is not affected by load condition and distributed capacitance. This paper also proposes a time synchronization method based on the Tellegen's quasi-power theorem to calculate and correct the time synchronization error. Therefore, the proposed pilot protection has a high synchronization accuracy and has no requirement on the communication delay. In this paper, different simulation models are established by using MATLAB/Simulink and PSCAD and extensive simulation studies verify the effectiveness of the proposed protection approach and time synchronization method.**

***Index Terms*-- Tellegen's quasi-power theorem, Differential protection, Ultra-high voltage, Protection relay**

I. Introduction

CURRENT differential protection has many advantages such as simplicity and high reliability, and thus it has been widely used in power system [1-5]. As current differential protection is based on Kirchhoff's current law, the object to be protected must be an 'electrical node'. When it is applied to a transmission line, certain simplified assumptions are required, however, which bring problems. For examples, synchronous sampling of currents at the two ends of the transmission line is required, and the sensitivity of protection is affected by load current and distributed capacitive current. Many works have been done to improve the performance of current differential protection. Unfortunately, solutions presented in literatures may overcome the shortcomings but sacrifice some of the advantages of current differential protection at the same time.

To eliminate the effect of distributed capacitive current, references [6-8] propose methods based on calculation and compensation of the capacitive current in differential current. Most of commercial protection devices consider only the static capacitive current [9,10]. However, during fault condition, the capacitive current changes significantly due to the drastic variation in voltage. References [11-14] present methods to calculate and compensate the transient capacitive current. In commercial relays of GE and SEL, they calculate the capacitive current according to the instantaneous voltages at the terminals of transmission line. The zero-sequence capacitive current cannot be well compensated under some conditions. In relays of ABB, zero sequence capacitive current is also considered in the accurate compensation method. However, when a tap transformer or shunt reactor is included in the protected zone, the approximate compensation method should be used instead. Besides, the compensation methods in these commercial relays are based on lumped parameter model, which brings error for a very long transmission line [14]. These methods are greatly affected by the transient process of the voltage transformer, and they need the parameters of distributed capacitance of the line to calculate the capacitive current. If consider changes in the parameters of capacitance or shunt reactor, these protection methods will become more complicated.

In order to solve the problem of sampling synchronization, current differential protection relays for transmission lines mostly adopt 'ping-pong' method based on the calculation of communication delay, or time synchronization methods based on global satellite systems such as GPS and Beidou system [15,16]. As the 'ping-pong method' assumes that the delays of sending and receiving data in communication channel are equal, it cannot be used in a communication network. The GPS-derived time reference required for channel asymmetry compensation is brought into the GE' L90 relay via a regular IRIG-B input. Though this method allows multiple units to share a single GPS system to save cost, it is still a solution applying GPS for auxiliary synchronization. To ensure the effectiveness of the IRIG-B signal, meeting the accuracy requirements of 250 microseconds, the cost of such a system is not cheap. The time synchronization method based on satellite system increases the difficulty and investment of project implementation.

This work was supported by the National Natural Science Foundation of China under Grant 51677108. The proposed Tellegen's quasi-power protection has been applied for a Chinese patent (ZL 201510778144.4).

S. M. Liu, B. Wang, and Y.S. Zhao are with the Key Laboratory of Power System Intelligent Dispatch and Control of Ministry of Education, Shandong University, Jinan 250061, Shandong Province, China (e-mail: lsm@sdu.edu.cn).

L. L. Zhang is with School of Electric Power Engineering, South China University of Technology, Guangzhou 510640, Guangdong, China (e-mail: epzhangll@scut.edu.cn).

L. Jiang is with the Department of Electrical Engineering and Electronics, University of Liverpool, Liverpool, U.K. (e-mail: ljiang@liv.ac.uk).

In recent years, researchers have proposed protection schemes based on power [17] and energy [18,19] differential, which require both voltage and current phasors. Where power is calculated as the conjugate multiplication of phasors, and energy is calculated as the integration of instantaneous power to eliminate the influence of synchronization factors. Subsequently, the main problem of power differential and energy differential is affected by the voltage. When a solid fault occurs at near end of line, no matter internal or external fault, the voltage measured at this end is close to zero. In this case, the calculated power difference is highly related to the power angle. With some specific power angles, the power differential cannot make full discrimination between internal and external faults [20]. A complementary aid is needed, which increases the complexity of power differential protection.

Improved traditional protection principles [21-27] and new pilot protection schemes based on impedance have also been proposed [28-31]. Although impedance-based methods do not require capacitive current compensation, they still have some drawbacks. In [25,26], the application of lumped parameter R-L model causes the inherent inaccuracy of the protection algorithm for a long-distance transmission line. In [25-30], the performance of the proposed protection schemes is affected by the system impedance. In [26-29], it is difficult to set thresholds for transient conditions and weak-infeed lines. The concept of virtual impedance is introduced in [30] which does not have a physical meaning. The proposed method is complex, and it is difficult to set threshold. The protection scheme presented in [31] has a dead zone, and thus it needs additional criterion, which increases the complexity.

In [32], the authors proposed a pilot protection scheme based on longitudinal tapped impedance which does not require compensation of capacitive current and considers the shunt reactor. However, the scheme still needs synchronization on the two ends of line. A pilot protection scheme based on two-port network model is presented in [33]. Since only the amplitudes of two-port network parameters are used for judgment, it is not affected by the asynchronous sampling. However, both these two methods require the parameters of the line impedance. Inaccurate line impedance parameter will affect the performance of protection scheme.

The motivation of this paper is to propose a method does not suffer from distributed capacitive current and asynchronous sampling, based on the Tellegen's quasi-power theorem. The contributions include:

1) It is pointed out that in two circuits that satisfy Tellegen's quasi-power theorem the branches with the same original parameters can be ignored in the calculation of quasi-power. Therefore, the calculation and comparison of quasi-power can be realized by using only the current and voltage at the terminals of the two circuits.

2) The current phasor instead of its conjugate is used for calculation of quasi-power. However, when the measured samples at the two ends of transmission line are not synchronized, it will cause error in the calculation. To solve this problem, a new time synchronization algorithm is proposed.

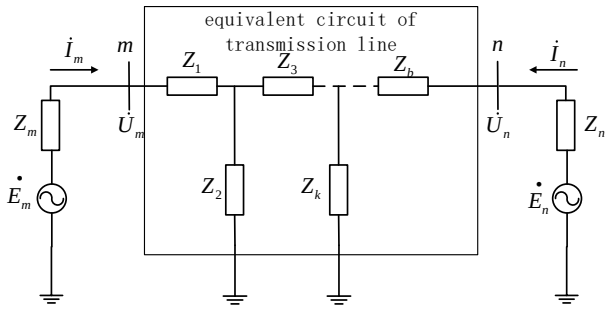

Fig. 1 Equivalent circuit of transmission line.

For a transmission line, different circuits can be constructed for different conditions, i.e., normal operation, external fault, and internal fault. In this paper, the Tellegen's quasi-power theorem is used to analyze the relationship between any two of these circuits. The quasi-power difference can be calculated and used to discriminate internal fault from normal operation and external fault. Since the branches representing distributed capacitive and shunt reactor also meet the requirements, they will not affect the discrimination of fault and the sensitivity of the protection. In addition, the quasi-power difference of transmission line is zero under normal load condition. Take advantage of this, the synchronization error at the two ends of transmission line can be calculated and corrected. Simulation results confirmed the effectiveness of the proposed scheme.

The organization of the rest of the paper is as follows: the proposed Tellegen's quasi-power protection and time synchronization method are described in Section II. Their effectiveness is validated in Section III with extensive comparison studies and visualizations. Finally, Section IV concludes the paper.

II. Tellegen's Quasi-Power Theorem based Pilot Protection

A. *Tellegen's Quasi-Power Theorem*

Tellegen's quasi-power theorem [34] is similar to Kirchhoff's current law, and it is not affected by the topology of circuit and the parameters of electrical components. Assume there are two circuits (hereinafter referred as circuit 1 and circuit 2), which have same graph (*n* nodes and *b* branches) but different parameters for branches. Denote the currents and voltages of *b* branches in the two circuits by $(i_1, i_2, \ldots, i_b)$, $(u_1, u_2, \ldots, u_b)$, $\left(\hat{i}_1, \hat{i}_2, \ldots, \hat{i}_b\right)$ and $\left(\hat{u}_1, \hat{u}_2, \ldots, \hat{u}_b\right)$, respectively. Assume the current and voltage of each branch take the associated reference direction, then at any time *t* we have

$$\sum_{k=1}^{b} u_k \hat{i}_k = 0 \text{ and } \sum_{k=1}^{b} \hat{u}_k i_k = 0 \tag{1}$$

For AC circuits, where the fundamental frequency current and voltage are represented by phasors, the Tellegen's quasi-power theorem is also applicable.

Fig. 1 shows a single-line diagram for the equivalent circuit of a transmission line. E_m and Z_m are the potential and impedance of equivalent system on the left, respectively. E_n and Z_n are the potential and impedance of the equivalent system on the right, respectively. Z_1~Z_k are the equivalent impedances of

the line. In Fig. 1, multiple T-type equivalent circuits are used to describe the transmission line. Note that other forms of equivalent circuit such as multi-π type and distributed parameter model can also be used, which will not affect the subsequent discussion of Tellegen's quasi-power theorem.

In Tellegen's quasi-power theorem, expressed in phasors, if the impedances of the *k*-th pair of branches in circuit 1 and circuit 2 are equal, then we have:

$$\dot{U}_k \hat{I}_k = \left(\dot{I}_k \cdot Z_k\right)\hat{I}_k = \dot{I}_k \cdot \left(Z_k \cdot \hat{I}_k\right) = \hat{U}_k \dot{I}_k \tag{2}$$

where *U* and *I* represent the phasors of voltage and current, respectively.

For an external fault, the structure and parameters of the transmission line are the same as that under normal operation condition. Therefore, the pre-fault positive sequence circuit and the post-fault positive sequence circuit of the transmission line can be treated as two circuits that satisfy Tellegen's quasi-power theorem. As the impedances of each pair of branches in the two circuits are equal, according to (2), we can get:

$$\begin{cases} \dot{U}_m \hat{I}_m + \dot{U}_n \hat{I}_n + \sum_{k=1}^{b} \dot{I}_k \hat{I}_k \cdot Z_k = 0 \\ \hat{U}_m \dot{I}_m + \hat{U}_n \dot{I}_n + \sum_{k=1}^{b} \hat{I}_k \dot{I}_k \cdot Z_k = 0 \end{cases} \tag{3}$$

where the superscripts $\cdot$ and $\hat{}$ represent pre-fault positive sequence phasor and post-fault positive sequence phasor, respectively. Considering that the positive-sequence and negative-sequence parameters of the transmission line are equal, for an asymmetric fault, (3) can also be applied to the positive-sequence equivalent circuit and the negative-sequence equivalent circuit.

For (3), by subtracting the second formula from the first, we have:

$$\left(\dot{U}_m \hat{I}_m + \dot{U}_n \hat{I}_n\right) - \left(\hat{U}_m \dot{I}_m + \hat{U}_n \dot{I}_n\right) = 0 \tag{4}$$

When an internal fault occurs, the fault branch, denoted by *f*, is added to the circuit. The current of this branch before the fault is 0, then the subtraction of the two formulas in (3) gives:

$$\left(\dot{U}_m \hat{I}_m + \dot{U}_n \hat{I}_n\right) - \left(\hat{U}_m \dot{I}_m + \hat{U}_n \dot{I}_n\right) = -\dot{U}_f \hat{I}_f \tag{5}$$

The voltage at any point on the transmission line before fault inception is close to the rated value, and the post-fault current of the fault branch is quite large. Therefore, the magnitude of the calculation result of formula (5) will be significant.

For multi-terminated line, the generalized form of (3) is

$$\begin{cases} \sum_{k=1}^{t} \dot{U}_k \hat{I}_k + \sum_{k=1}^{b} \dot{I}_k \hat{I}_k \cdot Z_k = 0 \\ \sum_{k=1}^{t} \hat{U}_k \dot{I}_k + \sum_{k=1}^{b} \hat{I}_k \dot{I}_k \cdot Z_k = 0 \end{cases} \tag{6}$$

where *t* is the number of terminals.

B. Tellegen's Quasi-Power Protection

Denote the quasi-power difference, the expression in the left side of (4) and (5), as $\dot{S}_{\mathrm{qd}}$, we have:

$$\dot{S}_{\mathrm{qd}} = P_{\mathrm{qd}} + jQ_{\mathrm{qd}} \triangleq \left(\dot{U}_m \hat{I}_m + \dot{U}_n \hat{I}_n\right) - \left(\hat{U}_m \dot{I}_m + \hat{U}_n \dot{I}_n\right) \tag{7}$$

By comparing (4) and (5), it can be known that the value of $\dot{S}_{\mathrm{qd}}$ is 0 for normal condition and external faults while it will be large for internal faults. On this basis, a new unit pilot protection can be formed, named Tellegen's quasi-power protection, or TQP protection for short.

Similar to the above derivation process for two terminals line, we have the generalized form of (7) for multi-terminal line as

$$\dot{S}_{\mathrm{qd}} = P_{\mathrm{qd}} + jQ_{\mathrm{qd}} \triangleq \sum_{k=1}^{t} \dot{U}_k \hat{I}_k - \sum_{k=1}^{t} \hat{U}_k \dot{I}_k \tag{8}$$

Since the calculation of quasi-power difference is affected by factors such as measurement error and calculation error, the value of $\dot{S}_{\mathrm{qd}}$ will not be zero and thus need to set a threshold to discriminate internal faults for disturbances. For internal fault, the apparent quasi-power difference $\dot{S}_{\mathrm{qd}}$ is mainly determined by the transient impedance of the fault branch, while in the case of external fault $\dot{S}_{\mathrm{qd}}$ is mainly determined by the calculation error due to harmonics. From the derivation process of (4), it can be known that the quasi-power difference $\dot{S}_{\mathrm{qd}}$ is not affected by load condition and distributed capacitance, etc. Therefore, when the through current is small and thus there is no CT saturation problem, a relatively low threshold can be chosen to increase the sensitivity. For a severe fault such as solid phase-phase fault or line-to-ground fault, very large through current may occur and result in CT saturation. The TQP protection adopts a larger threshold and thus has stronger tolerance to CT saturation.

The thresholds are set as follows:

$$\begin{cases} \begin{cases} |P_{\mathrm{qd}}| > P_{\mathrm{set}} = (0.05 \sim 0.08) S_{\mathrm{N}} \\ |Q_{\mathrm{qd}}| > Q_{\mathrm{set}} = (0.05 \sim 0.08) S_{\mathrm{N}} \end{cases}, & \dfrac{|I_m| + |I_n|}{2} \le 2I_{\mathrm{N}} \\ \begin{cases} |P_{\mathrm{qd}}| > P_{\mathrm{set}} = (0.5 \sim 0.6) S_{\mathrm{N}} \\ |Q_{\mathrm{qd}}| > Q_{\mathrm{set}} = (0.5 \sim 0.6) S_{\mathrm{N}} \end{cases}, & \dfrac{|I_m| + |I_n|}{2} > 2I_{\mathrm{N}} \end{cases} \tag{9}$$

where S_{N} and I_{N} represents the rated power and current of the transmission line, respectively. The low thresholds consider 2%-4% measurement and calculation error in voltage and current. The high thresholds consider large error due to factors like CT saturation, which can be over 20%.

As can be seen in Fig. 1, changes to parameters of the transmission line may affect the performance of the TQP protection. For example, the dynamic change of the FACTs will result in different impedances. The normal adjustment of FACTs will produce a small quasi-power difference which has little effect on TQP protection. However, the abrupt changes in parameters and states of FACTs will result in a large quasi-power difference and thus may cause TQP protection to malfunction. On the other hand, changes to the elements at terminals, such as week infeed, open circuit breaker and nonlinear loads, will not affect the adaptability of the TQP protection, as the structure and parameters of the line remain unchanged and the Tellegen' quasi-power theorem is still stratified.

C. Time Synchronization Method

In the derivation of formulas (3) to (5), in order to eliminate the influence of the internal impedance of the equivalent circuit of the transmission line, the calculation of the power does not use the conjugate of the current phasor. If the data measured at both ends of the transmission line is not synchronized, there will be a fake power difference, which will affect the judgment of the TQP protection. To avoid maloperation, this paper proposes a time synchronization method based on Tellegen's quasi-power theorem.

Here, consider the equivalent circuit of the transmission line under normal operating condition as circuit 1 and denote the voltage and current phasors at the two ends of line as $\dot{U}_m, \dot{I}_m, \dot{U}_n, \dot{I}_n$, respectively. Consider the equivalent circuit of the transmission line when an external fault occurs as circuit 2 and denote the current and voltage phasors at the two ends of line as $\hat{U}_m, \hat{I}_m, \hat{U}_n, \hat{I}_n$, respectively. These two circuits have the same topology and branch impedance. According to the Tellegen's quasi-power theorem, we can know that these phasors satisfy (4).

When the data sampling at the two ends of transmission line is not synchronized, taking the m side as reference, the measured phasor at the n side can be equivalent to the actual phasor shifted by an angle corresponding to the time synchronization error. It can be expressed as:

$$\begin{aligned} &\left(\dot{U}_m \hat{I}_m + \dot{U}_n \hat{I}_n e^{-j\theta}\right) - \left(\hat{U}_m \dot{I}_m + \hat{U}_n \dot{I}_n e^{-j\theta}\right) = 0 \\ &\Rightarrow \left(\dot{U}_n \hat{I}_n e^{-j\theta} - \hat{U}_n \dot{I}_n e^{-j\theta}\right) = \left(\hat{U}_m \dot{I}_m - \dot{U}_m \hat{I}_m\right) \\ &\Rightarrow e^{-j\theta} = \left(\hat{U}_m \dot{I}_m - \dot{U}_m \hat{I}_m\right) / \left(\dot{U}_n \hat{I}_n - \hat{U}_n \dot{I}_n\right) \end{aligned} \tag{10}$$

For normal operation conditions and external faults, the shifted angle can be obtained according to (10), and can be used to calculate the corresponding time synchronization error. Afterwards, we can adjust the sampling time on the n side according to the calculated time synchronization error, to achieve synchronous sampling at the two ends of line. Similarly, we can also take n side as reference and adjust the sampling time of phasors at the m side.

Equation (10) uses the electrical quantities at the two ends of line to calculate the time synchronization error, which is not affected by the inconsistency of the transmission and reception delay of the communication channel. Compared with the 'ping-pong' method used in current differential protection which requires equal transmission and reception delays, the proposed time synchronization method has better adaptability.

From the perspective of solving equation, the greater the difference between the two sets of voltage and current phasors in (10), the better the solution and the ability to tolerate error and noise. Therefore, the voltage and current phasors under the normal operation conditions and external faults are employed. Before the TQP protection is implemented, a data set can be initialized by using simulated phasors. After that, the data set are updated by using measured phasors.

The complete process of TQP protection is shown in the Fig. 2. At first, calculate the superimposed current, Δi, i.e., subtract the sample of current at present moment with the sample measured at the time instant just one cycle before. If Δi is not larger than 0.2 times of the rated current, I_N, then update the historical data with the measured samples. On the other hand, if Δi is larger than $0.2I_N$, a fault (external or internal) will be detected and to be discriminated in the next step. Fetch the historical data of phasors measured under normal operation and external fault conditions, and use them to calculate the time synchronization error according to (10). After the samples of voltage and current have been adjusted according to the calculated time synchronization error, calculate $\dot{S}_{qd}$ according to (7). If both of P_{qd} and Q_{qd} are not larger than the corresponding thresholds, the fault will be judged as external fault, and then update the historical data with the measured samples. If at least one of P_{qd} and Q_{qd} is larger than the corresponding preset threshold, the fault will be identified as an internal fault. Then, conduct faulted phase selection and trip the faulted phase(s).

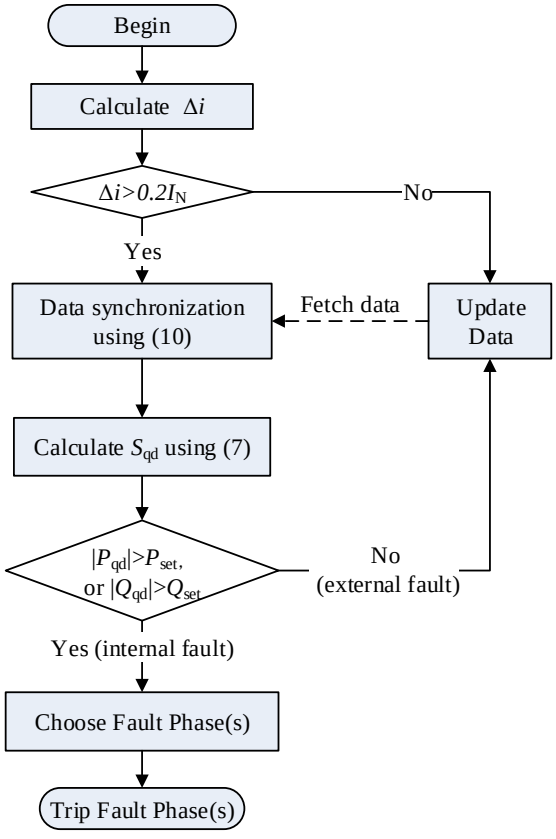

Fig. 2 The flowchart of the proposed TQP protection scheme.

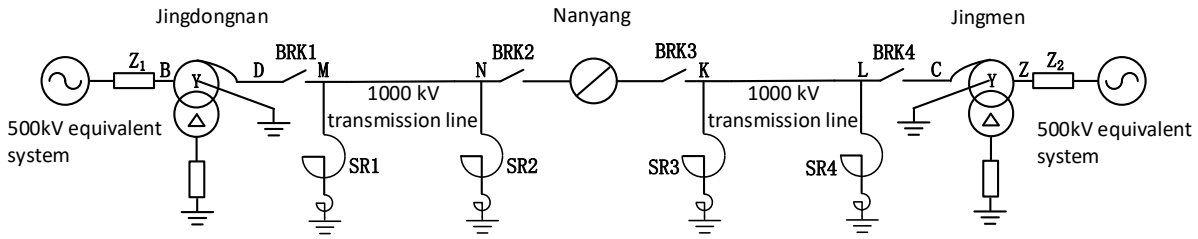

Fig. 3. Simulation model of an ultra-high voltage transmission line installed in China.

III. CASE STUDIES

To verify the performance of the TQP protection, a simulation model for the ultra-high voltage (UHV) demonstration project in China is built, as shown in Fig. 3. The project has a 1000 kV 654 km transmission line, from Jindongnan substation in Shanxi province to Jingmen substation in Hubei province. The switch station in Nanyang, Shanxi divides the whole line into two parts, namely Jindongnan-Nanyang line (J-N line, 363km) and Nanyang-Jingmen line (N-J line, 291km). The power grids at the sending end (Jindongnan) and the receiving end (Jingmen) are equivalent to two 500 kV power sources. The equivalent parameters of the transmission line and power sources can be seen in Appendix A in [33].

The rated power transmission capacity of the demonstration project is 2800MW, and the thresholds of the TQP protection are set as:

$$\begin{cases} \begin{cases} P_{\text{set}} = 0.08 \times S_N = 224\text{MW} \\ Q_{\text{set}} = 0.08 \times S_N = 224\text{Mvar} \end{cases}, & \dfrac{|\mathrm{I}_m| + |\mathrm{I}_n|}{2} \le 2I_N = 3600A \\ \begin{cases} P_{\text{set}} = 0.5 \times S_N = 1400\text{MW} \\ Q_{\text{set}} = 0.5 \times S_N = 1400\text{Mvar} \end{cases}, & \dfrac{|\mathrm{I}_m| + |\mathrm{I}_n|}{2} > 2I_N = 3600A \end{cases} \tag{11}$$

In the following, J-N line is treated as the protected line. In other words, a fault occurred on J-N line will be treated as internal fault while a fault occurred on N-J line are treated as external fault.

TABLE I
Power difference under different potential angles

Potential angle difference	Power difference with shunt reactor (MW)	Power difference without shunt reactor (MW)	Quasi-power difference （MW）
0°	268.14	2231.0	4.95
10°	232.50	2176.2	4.80
30°	35.89	1790.0	4.47
45°	387.43	1282.7	4.34
60°	846.39	626.65	4.07

A. Influence of Distributed Capacitive Current

For an EHV/UHV transmission line, the distributed capacitance is very large. Subsequently, the capacitive current will reduce the sensitivity of differential protection, and the capacitive reactive power will reduce the sensitivity of traditional power differential protection. In the TQP protection, because the distributed capacitance branch satisfies (2), the quasi-power difference will also be 0 under normal operation condition, therefore, the TQP protection is not affected by the distributed capacitance.

Taking the UHV demonstration project as an example, the magnitude of the capacitive current of J-N line can reach 1318 A, which is 73.22% of the rated current. After compensation by using shunt reactor, the magnitude of the capacitive current can still reach 162.67 A. To avoid maloperation, the current differential protection must raise the threshold to above level of the capacitive current. However, this will reduce the sensitivity of traditional power differential protection. Traditional current differential protection can only detect faults with the transient fault resistance less than 200 Ω, which is much lower than the requirement (600 Ω) [33]. Additional measures need to be implemented, however, which increase the complexity.

The sensitivity of traditional power differential protection will also be affected by the reactive power generated by the distributed capacitance. Table I lists the power difference between the two ends of transmission line under different load conditions. Column 2 and 3 show the power difference between the two ends for the cases with/without shunt reactor, respectively. For comparison, the table also gives the values of quasi-power difference.

It can be seen from the table that the power difference varies greatly under different load conditions. The shunt reactor also has a great influence on the power difference, indicating that the distributed capacitance has a great influence on the power difference. The threshold value of traditional power differential protection must be able to avoid the maximum distributed capacitive power, for example, 1000 MW. Under light load conditions, the power differential protection can only detect fault with transient resistance about 300 Ω. By dynamically adjusting the threshold according to the magnitude of the load current can improve the sensitivity of the protection to a certain extent, but it is still difficult to meet the requirement of 600 Ω. Besides, it can also be seen that the impact of shunt reactor is huge. When an internal fault occurs, the power difference may be even less than the power difference under load conditions.

In contrast, the calculated values of the quasi-power difference are always less than 5 MW for all the cases shown in Table I. The values are very close to 0 and the deviation is caused by calculation error, which is consistent with the above theoretical analysis. Different cases without shunt reactor have also been simulated, and the calculated values of the quasi-power difference does not exceed 5 MW either. These results confirm that the proposed TQP protection is not affected by distributed capacitance and the status of shunt reactor. In fact, all static components in the protected zone will not affect the performance of the proposed TQP protection.

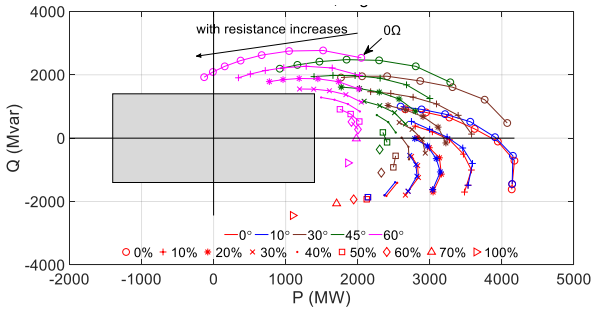

(a) internal faults with high current

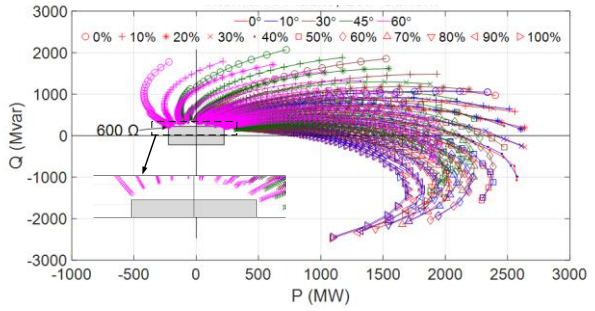

(b) internal faults with low current

Fig. 4. The effect of transient resistance (internal faults)

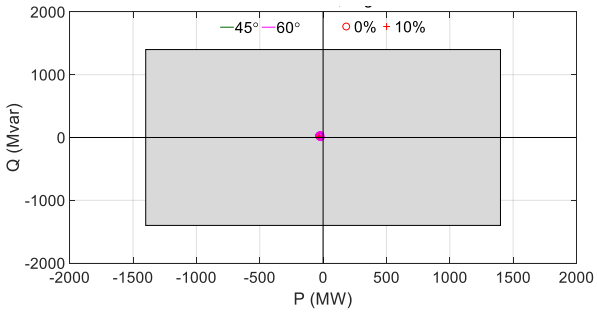

(a) external faults with high current

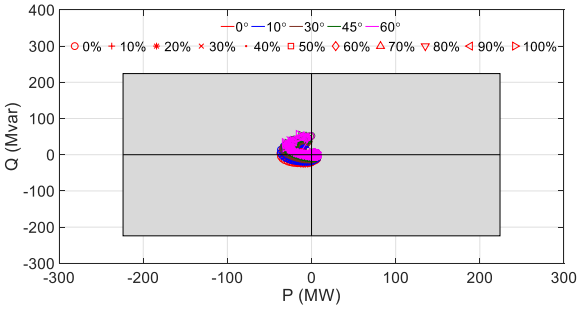

(b) external faults with low current

Fig. 5. The effect of transient resistance (external faults)

B. Influence of Transition Resistance

When a single-phase-to-ground fault occurs on the transmission line, there may be transient resistance caused by wooden poles, gravel, and branches in the fault circuit, which requires that the protection has high sensitivity. At the beginning stage of the fault, high order harmonics and noise in the voltage and current will have a large impact on the calculation of $\dot{S}_{qd}$. To simulate this situation, the data measured in a fundamental frequency cycle right after the fault is used for calculation, and a 26 dB Gaussian white noise is added to the simulation data.

Fig. 4 shows the results of the TQP protection for single-phase-to-ground faults with transient resistance varies from 0 to 600 Ω. The setting of phase angle difference between the two sources includes 0°, 10°, 30°, 45° and 60°, and the fault location is changed from 0% to 100% at a step of 10% on the J-N line.

In the figures, 5 different colors represent 5 different phase angle differences. For instances, the curves in red are obtained when the phase angle difference is 0° while the curves in purple are obtained when the potential angle difference is 60°. For each phase angle difference, there may be 11 curves with the same color but different markers, corresponding to 11 different fault locations as indicated in the legend. Different points in a curve correspond to different transient resistances which arrange counterclockwise with the fault resistance increases. The rectangular area in gray represents the restraint zone of the proposed TQP protection. This is to say, a point locates outside the area means the TQP protection will trips for the corresponding case.

Fig. 4(a) shows the results of the faults with low transition resistance. According to (9), the current is larger than $2I_N$ and thus the TQP protection adopts the large thresholds for these cases. Fig. 4(b) shows the results of the faults with high transition resistance, for which low thresholds are adaptively selected for the TQP protection due to the low current level. For examples, the points at the rightest side of the curves in purple in Fig. 4(a) corresponds to 0 Ω while in Fig. 4(b) the points close to the rectangle box correspond to 600 Ω.

We can see from Fig. 4 that the proposed TQP protection can identity and trip all the internal faults with transition resistance up to 600 Ω under various load conditions and fault locations. On the other hand, we can see from Fig. 5 that all the external faults are restrained by the TQP protection. By adaptively selected the thresholds, the TQP protection has high sensitivity for high resistance internal faults and high reliability for external faults.

To save page and for the convenience to see how the quasi-power changes under different fault conditions, even though high/low thresholds may be selected for the following test cases, the results are shown in the same figure and only the boundary corresponding to the low thresholds will be displayed.

C. Influence of Different Fault Types

In Fig. 4 and 5, only single-line-to-ground faults are considered. To further verify the performance of TQP protection, its operating characteristics for different types of multi-phase faults is further analyzed.

Fig. 6 shows the results of TQP protection when multi-phase internal faults occur on the J-N line. Fig. 6(a) shows the results of phase-to-phase (BC) faults under different conditions where the transient resistance is from 0 to 50 ohms. Fig. 6(b) shows the results of two-phases-to-ground faults (BCN) under different conditions, where the grounding resistance are 0 and transient resistance between two phases are from 0 to 50 Ω. Fig. 6(c) shows the results of two-phases-to-ground faults (BCN) where the transient resistance between phases is fixed to 5 Ω and the transient grounding resistance is from 0 to 600 Ω. Fig. 6(d) shows the result of three-phase short-circuit faults (ABC), where the transient resistance is from 0 to 50 Ω.

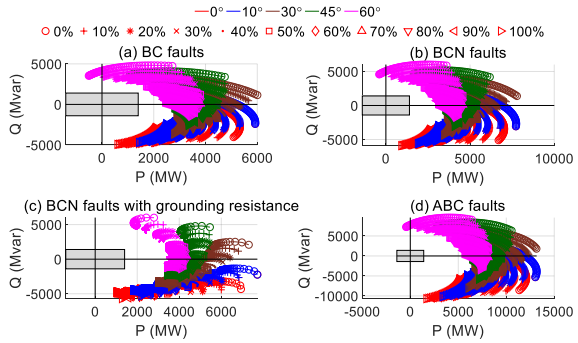

Fig. 6. Operation of TQP protection for multi-phase faults on J-N line

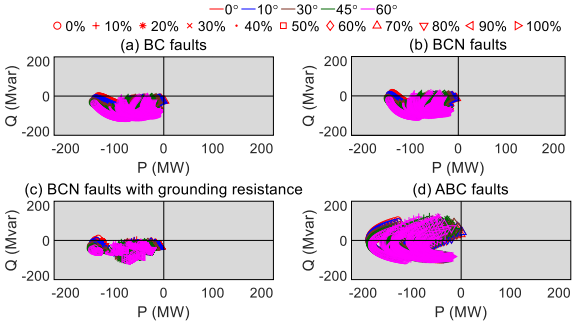

Fig. 7 Operation of TQP protection for multi-phase faults on N-J line.

As shown in the four subfigures, the quasi-power differences are all far from the restrained zone in all cases. This is because the multi-phase fault is more serious than the single-phase high-impedance grounding fault. This means the proposed TQP protection can accurately identify different types of internal faults with high sensitivity.

Fig. 7 shows the operation of the TQP protection when external faults occur on the N-J line. Each subfigure here shows the results of a type of faults, and the fault conditions are the same as that in Fig. 6 except fault location. From the figures, we can see that the quasi-power differences for all the cases are within the rectangle restraint zone and keep away from the boundary. This means that the proposed TQP protection can accurately identify various external faults with high reliability.

D. Influence of CT Saturation

In order to evaluate the influence of CT saturation on the TQP protection, a 230kV transmission system with the JA model of current transformer built in PSCAD is employed. Different degrees of saturation are simulated by changing the secondary resistance (R_g) of the current transformer. The larger the secondary resistance, the severer the saturation. Short-circuit external faults are applied to study the operation of the protection when the CT is saturated.

For the cases with large current, where CT saturation may occur, the TQP protection adopts the large thresholds (50W + j*50Var, converted to the secondary side). As shown in Fig. 8(a), with increase of the value of R_g, the TQP protection enters the trip zone from the restraint zone, because the severity of CT saturation increases. For single-line-to-ground fault, the TQP protection can withstand high secondary resistance up to 119 Ω. The corresponding current waveform is shown in Fig. 8(b) where the starting time of CT saturation is about 6.7ms after the fault. For a three-phase fault, the TQP protection can correctly response to the fault when secondary resistance is up to 71.5 Ω. In contrast, for the current differential protection, it enters the trip zone when R_g are 22 Ω and 18 Ω for these two cases, respectively. Therefore, the tolerance of the TQP protection to CT saturation is much better than the conventional current differential protection.

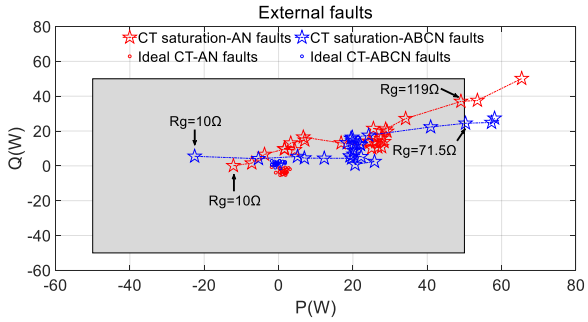

(a) Influence of CT saturation severity (Rg) on the TQP protection

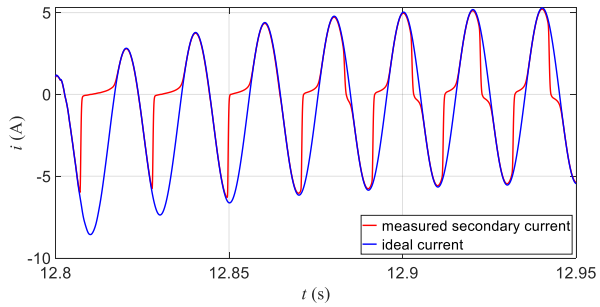

(b) the ideal and the measured secondary current (Rg=119 Ω))

Fig. 8. The operation of the TQP protection considering CT saturation

E. Influence of Inaccuracy in Voltage Measurement

As the proposed method uses voltage and current at both ends of line, inaccuracies in voltage measurement should also be considered. Taking an external solid single line-to-ground fault as example, the voltage waveform is shown in Fig. 9, with the ideal voltage in blue and the secondary voltage of CVT in red. Fig. 9(a) corresponds to fault inception angle 0° while Fig. 9(b) corresponds to fault inception angle 90°. It can be seen that the secondary voltage of CVT deviates from the ideal value during the transient process.

Fig. 10 shows the operation of the TQP protection during transient process considering the inaccuracy in voltage measurement. In the figure, red markers correspond to the results at different time instant with the potential angle of 0°. Similarly, green to 10°, blue to 30°, black to 45°, and yellow to 60°. As can be seen from the figure, the results for these cases are all within the range of 8W+j*8Var, converted to the secondary side, indicating that inaccuracies in voltage measurement due to the transient process of CVT do not cause maloperation of the TQP protection.

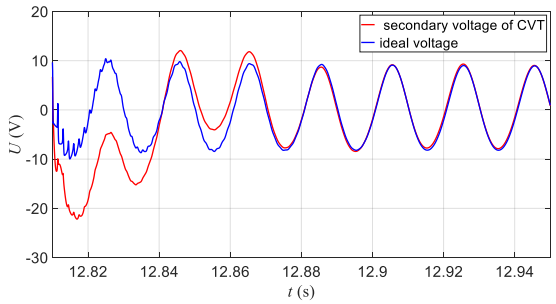

(a) the fault inception angle is 0°

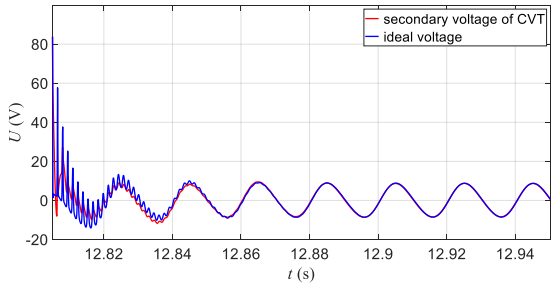

(b) the fault inception angle is 90°

Fig. 9. The ideal voltage and secondary voltage of CVT

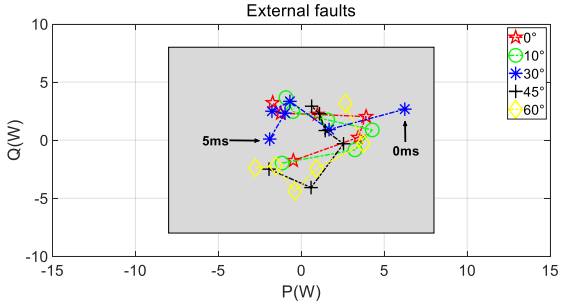

Fig. 10 The operation of the TQP protection considering the impact of CVT

F. *Influence of Power Swing*

During power swing, the equivalent circuit of transmission system still satisfies the Tellegen's quasi-power theorem. However, the variation in frequency during power swing will bring errors to the calculation of current and voltage phasor.

Fig. 11 shows the waveforms of voltage and current during a power swing with the frequency of 1Hz. The quasi-power difference can be calculated by using the current and voltage at normal operation and the current and voltage during power swing. The results in a 2s period are shown in Fig. 12. It can be seen that during power swing the quasi-power difference value is within the restraint zone so that the TQP protection will not malfunction.

G. *Synchronization Method Error Analysis*

Conventional power calculation uses the conjugate multiplication of voltage phasor and current phasor, thereby it can eliminate the effects of asynchronous sampling at the two ends of transmission line. However, to make the quasi-power of the internal branches to be zero, calculation of quasi-power according to (3) directly uses the current phasor instead of its conjugate. Therefore, when the measured samples at the two ends of transmission line are not synchronized, it will cause error in the calculation of the quasi-power difference according to (7) and affect the judgment of TQP protection.

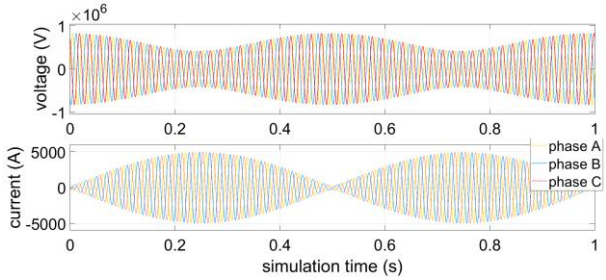

Fig. 11 The waveforms of voltage and current during a power swing

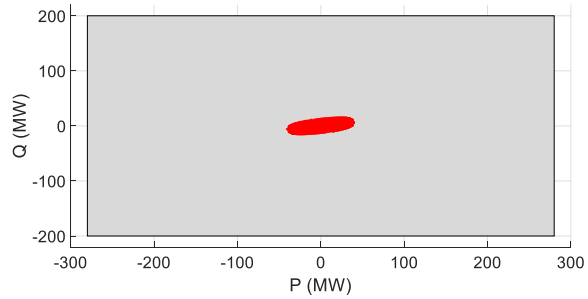

Fig. 12 The calculated results of quasi-power during a power swing

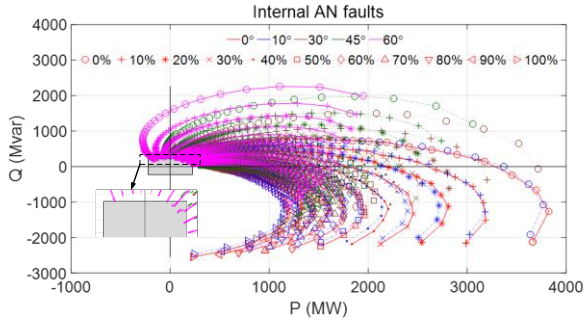

(a) The time synchronization error is 1 ms

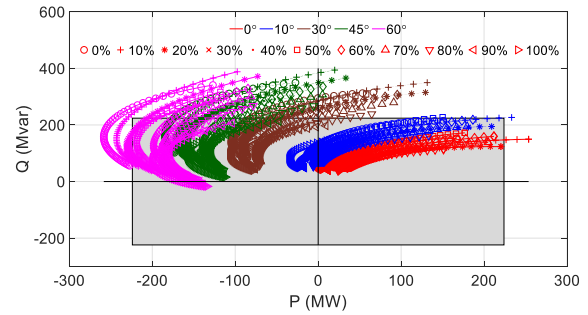

(b) The time synchronization error is 0.3 ms

Fig. 13. The results of test cases considering time synchronization error

Without correction to the asynchronous sampling, when the time error at the two ends of J-N line exceeds 1 ms, TQP protection may fail to operation for some internal faults, such as a single-phase-to-ground fault with high resistance as shown in Fig. 13(a). For external faults, such as a three-phase short-circuit fault occurs on N-J line, if the time synchronization error at both ends of J-N line reaches 0.3 ms, the TQP protection may maloperation, as shown in Fig. 13(b).

When the TQP protection determines that the line is not faulty, the voltage and current phasors are recorded as one set of data under normal operating condition. The current and voltage phasors measured at both ends of the J-N line, during

the external fault (fault on N-J line), are recorded as the other set of data. Here, samples from the tenth cycle after fault inception is used to calculate the voltage and current phasors, which help to eliminate the effects of harmonics and non-periodic components after the fault.

To evaluate the effectiveness of the time synchronization method, 11770 simulation cases have been conducted under different load conditions and external faults. The potential angle difference is set to 0°, 10°, 30°, 45° and 60° in different cases. The location of faults on N-J line vary from 0% to 100% at a step of 10%, and transient fault resistance varies from 0 to 600 Ω at a step of 10 Ω.

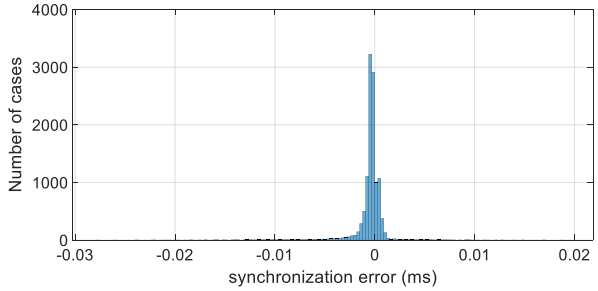

Fig. 14 Error analysis of time synchronization algorithm

The difference between the calculated results and the actual time synchronization error are shown in Fig. 14. From the figure, we can find that for most of cases the differences between the calculated time synchronization errors and actual values are in the range of [-0.005 +0.005] ms. The maximum positive error is 0.0195 ms and the maximum negative error is -0.0278 ms, which are much smaller than the values that may cause the TQP protection to malfunction. Therefore, the proposed time synchronization method is very effective and can ensure the TQP protection to act correctly.

H. The Speed of the TQP Protection

The TQP protection uses the superimpose component of current to detect disturbance and the start-up threshold is 0.2 I_N. The full cycle Fourier transform is then used to calculate the phasors of current and voltage. Therefore, the delay of the TQP protection is the fault detect time plus 1 cycle.

Considering different load conditions, fault types, fault locations, fault inception angles, transient resistances, etc., a total of 58,850 cases were simulated. The results are shown in Fig. 15, where the minimum delay is 20.1ms and the maximum delay is 22.45ms. The speed of the TQP protection is comparable to that of traditional current differential protection.

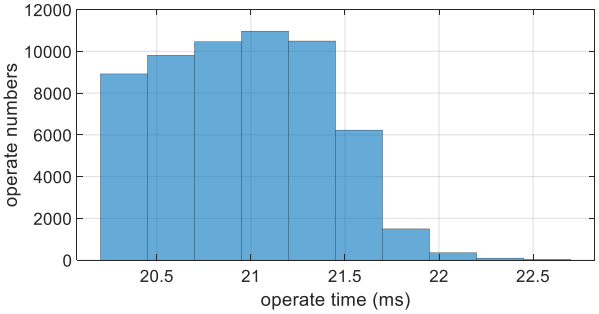

Fig. 15. The speed of the TQP Protection

TABLE II
Comparison of TQP and RCD protection considering phasor error

Phase error	Rate of misoperation for internal faults (%)			Rate of malfunction for external faults (%)		
	TQP	RCD1	RCD2	TQP	RCD1	RCD2
3%	0.47	9.28	28.45	2.1250	0	0
5%	0.76	9.07	28.34	7.88	0	0
10%	1.45	8.63	27.87	24.23	0.17	0

TABLE III
Comparison of TQP and RCD protection considering CT saturation

Rg (Ohm)	Rate of misoperation for internal faults (%)			Rate of malfunction for external faults (%)		
	TQP	RCD1	RCD2	TQP	RCD1	RCD2
10	0	0	25.13	0.27	20.87	0
20	0	0	25.19	0.27	21.85	0
70	0	0	25.30	0.76	21.80	0.71
120	0	0	25.79	1.80	20.40	6.50
450	7.10	0	25.84	41.20	41.31	39.24

I. Comparison Studies

In order to evaluate the dependability and security of the proposed method, extensive simulation studies were conducted considering CT saturation and phasor error, compared with the conventional restraint current differential (RCD) protection. A low threshold (0.2 I_N) and a high threshold (0.4I_N) are set for the starting current, respectively. The inflection point current is 0.8 I_N, and the restraining slope is 0.4.

33600 cases with faults on J-N line (internal fault) or N-J line (external fault) were conducted. The fault types include single-line-to-ground fault and three-phase short circuit fault. The fault locations include the midpoint and the two ends of the line. The transition resistance in grounding fault is between 0~600 Ω and transition resistance in three-phase fault is between 0~50 Ω. Five different levels of load conditions are considered.

Considering different levels of phasor error, the percentage rates of the TQP protection to malfunction or misoperation are shown in the Table II, in compared with the results of the RCD protection. The RCD protection with low threshold and high threshold are denoted as RCD1 and RCD2, respectively. If the phasor error is less than 3%, the TQP protection barely has malfunction and misoperation. In contrast, the rates of RCD1 and RCD2 to misoperation are 9.28% and 28.45%, respectively. When the phasor error is large than 3%, the TQP protection also has higher reliability (smaller misoperation rate) than RCD protection, normally in the cases of single-phase high-resistance grounding fault. But in terms of security, the TQP protection has higher malfunction rate than the RCD protection. The reason is that voltage and current are multiplied to calculate quasi-power so that the influence of phasor error on the TQP protection is greater. Therefore, a filter algorithm with a longer time window can be considered to reduce the error in phasor calculation, but this will slow down the speed of protection. To show the regular pattern, phasor error up to 10% is consider in the simulation, however, it would not be so large in real application.

To evaluate the performance of the TQP protection under different conditions of CT saturation, 3660 simulation cases were conducted considering different fault types, fault locations and fault inception times. For each fault, 5 different secondary resistance of CT are simulated. The results are shown in Table III. When the secondary resistance is not larger than 120 Ω, both the TQP and RCD1 can act correctly to all the internal faults. Nevertheless, for external faults, the rate of malfunction of the TQP protection is much smaller than that of the RCD protection with low threshold (over 20%). By increasing the threshold, the malfunction rate of the RCD decreases while the misoperation rate rises significantly. If the secondary resistance is up to 450 Ω, both protection schemes have high rates of malfunction.

IV. Conclusion

This paper proposed a new pilot protection method based on the Tellegen's quasi-power theorem for transmission line. Theoretical analysis and simulation studies have shown that the proposed method is not affected by load conditions and distributed capacitance and thus it has very high sensitivity and reliability under various fault conditions.

Aiming at solving the sampling synchronization problem at the two ends of transmission line, a time synchronization method based on Tellegen's quasi-power has also been proposed in this paper. This method has no special requirements on the communication channel, and thus has better applicability. Simulation results has shown that it can accurately calculate the time synchronization error with the maximum absolute value smaller than 0.03 ms, which ensure the correct action of the proposed TQP protection.

The tolerances of the TQP protection to various conditions, such as CT saturation, transient process of CVTs, phasor error, etc., have been validated. The adaptability and solution of the TQP protection to FACT devices, multi-terminal transmission line and HVDC project will be further studied in the next step.

V. References

[1] P. M. Anderson, Power System Protection. New York: Wiley, 1998.

[2] X. Lin, Z. Li, K. Wu, and H. Weng, "Principles and implementations of hierarchical region defensive systems of power grid," *IEEE Trans. Power Del.*, vol. 24, no. 1, pp. 30–37, Jan. 2009.

[3] X. Lin, Q. Tian, and M. Zhao, "Comparative analysis on current percentage differential protections using a novel reliability evaluation criterion," *IEEE Trans. Power Del.*, vol. 21, no. 1, pp. 66–72, Jan. 2006.

[4] Z. Y. Xu, Z. Q. Du, L. Ran, Y. K. Wu, Q. X. Yang, and J. L. He, "A current differential relay for a 1000-kV UHV transmission line," *IEEE Trans. Power Del.*, vol. 22, no. 3, pp. 1392–1399, Jul. 2007.

[5] S. Dambhare, S. A. Soman, and M. C. Chandorkar, "Adaptive current differential protection schemes for transmission-line protection," *IEEE Trans. Power Del.*, vol. 24, no. 4, pp. 1832–1841, Oct. 2009.

[6] T. S. Bi, Y. L. Yu, S. F. Huang, and Q. X. Yang, "An accurate compensation method of distributed capacitance current in differential protection of UHV transmission line," in *Proc. IEEE Power Eng. Soc. Gen. Meeting*, San Francisco, CA, USA, vol. 2005, 2005, pp. 770–774.

[7] Y. Zhang and J. Suonan, "Phaselet-based current differential protection scheme based on transient capacitive current compensation," *IET Gener. Transmiss. Distrib.*, vol. 2, no. 4, pp. 469–477, Jul. 2008.

[8] H. Ito, I. Shuto, H. Ayakawa, P. Beaumont, and K. Okuno, "Development of an improved Smultifunction high-speed operating current differential relay for transmission line protection," in *Proc. 7th Int. Conf. Develop. Power Syst. Protection*, Amsterdam, Netherlands, 2001, pp. 511–514.

[9] *SIPROTEC 4 Line Differential Protection 7SD80 Manual, v4.7*, Siemens AG, Nürnberg, Germany, 2018.

[10] *Manual of CSC-213 Optical Fiber Differential Protection Relay and Measurement and Control Device*, Beijing Sifang Automation Co., Ltd., Beijing, China, 2006.

[11] L30 line current differential system instruction manual v7.7x, GE Multilin Inc., Markham, Ontario, 2018.

[12] *L90 Line Current Differential System Instruction Manual v7.7x*, GE Multilin Inc., Markham, ON, Canada, 2018.

[13] *Line Current Differential Protection Automation and Control System SEL-411L Datasheet*, Schweitzer Eng. Lab., Inc., Pullman, WA, USA, 2018.

[14] *Line Differential Protection RED670 IEC Technical Manual, Version 2.2*, ABB, Västerås, Sweden, 2017.

[15] D. L. Mills, "Internet time synchronization: The network time protocol," *IEEE Trans. Commun.*, vol. 39, no. 10, pp. 1482–1493, Oct. 1991.

[16] A. G. Phadke *et al.*, "Synchronized sampling and phasor measurements for relaying and control," *IEEE Trans. Power Del.*, vol. 9, no. 1, pp. 442–452, Jan. 1994.

[17] F. Oechsle, K. Feser, N. Schuster and L. Philippot, "Active power differential algorithm for protection of transmission lines," PowerTech Budapest 99. Abstract Records. (Cat. No.99EX376), Budapest, Hungary, 1999, pp. 207.

[18] M. M. A. Aziz, A. F. Zobaa, D. K. Ibrahim, et al. "Transmission lines differential protection based on the energy conservation law," *Electr. Power Syst. Res.*, vol.78, pp.1865-1872, 2008.

[19] D. T. Dantas, E. L. Pellini and G. Manassero, "Time-Domain Differential Protection Method Applied to Transmission Lines," *IEEE Trans. Power Del.*, vol. 33, no. 6, pp. 2634-2642, Dec. 2018.

[20] H. A. Darwish, A. M. I. Taalab and E. S. Ahmed, "Investigation of power differential concept for line protection," IEEE Trans. Power Del., vol. 20, no. 2, pp. 617-624, 2005.

[21] S. Hashemi, M.Tarafdar. "Transmission-line protection: A directional comparison scheme using the average of superimposed components", *IEEE Trans. Power Del.*, vol. 28, no. 2, pp. 955-964, 2013.

[22] J. Tan, D. Tholomier, B. Gu, et al, "Sensitivity and stability of superimposed component based directional comparison protection", *Proc. Can. Conf. Elec. and Computer Eng.*, pp. 280–283, 2007.

[23] B. Wang, X. Dong, Z. Bo. "Negative-sequence pilot protection with applications in open-phase transmission lines", *IEEE Trans. Power Deliv.*, vol. 25, no. 3, pp. 1306-1313, 2010.

[24] X. Lin, S. Ke, Y. Gao, et al. "A selective single-phase-to-ground fault protection for neutral un-effectively grounded systems", *Electrical power and energy systems*, vol. 33, no. 4, pp. 1012-1017, 2011.

[25] J. Suonan, K. Liu, G. Song. "A novel UHV/EHV transmission line pilot protection based on fault component integrated impedance", *IEEE Trans. Power Deliv.* Vol.26, no. 1, pp. 127-134, 2011.

[26] J. Xia, X. Deng, L.Wang. "Enhanced transmission line pilot impedance and pilot protection", *IET Gener. Trans. Distr.*, vol. 5, no. 12, pp. 1240-1249, 2011.

[27] J. Suonan, X. Deng, K. Liu. "Transmission line pilot protection principle based on integrated impedance", *IET Gener. Trans. Distr.*, vol. 5, no.10, pp. 1003-1010, 2011.

[28] S. He, J. Suonan, Z. Bo. "Integrated impedance-based pilot protection scheme for the TCSC-Compensated EHV/UHV transmission lines", *IEEE Trans. Power Deliv.*, vol. 28, no. 2, pp. 835-844, 2013.

[29] J. Xia, J. Suonan, G. Song, et al, "Transmission line individual phase impedance and related pilot protection", *Electrical Power and Energy Systems*, vol. 33, no.9, pp. 1563-1571, 2011.

[30] J. Ma, P. Pei, W. Ma, et al, "A new transmission line pilot differential protection principle using virtual impedance of fault component", *Canadian Journal of Electrical and Computer Engineeing*, vol. 38, no.1, pp. 37-44, 2015.

[31] T. G. Bolandi, H. Seyedi, S. Hashemi, et al, "Impedance-differential protection: A new approach to transmission-line pilot protection", *IEEE Trans. Power Deliv.*, vol. 30, no. 6, pp. 2510-2518, 2014.

[32] S. Liu, J. Li, J. Wu, T. Guo and L. Jiang, "Ultra-high voltage/extra-high voltage transmission-line protection based on longitudinal tapped impedance," *IET Gener. Trans. Distr.*, vol. 11, no. 17, pp. 4158-4166, 2017.

[33] S. Liu, L. L. Zhang, C. Fu and L. Jiang, "A New Two-Port Network Model-Based Pilot Protection for AC Transmission Lines," *IEEE Trans. Power Del.*, vol. 35, no. 2, pp. 473-482, April 2020.

[34] B. D. H. Tellegen, "A general network theorem with applications" in Philips Research Reports, Eindhoven:Philips Research Laboratories, vol. 7, pp. 259-269, 1952.